Optik - International Journal for Light and Electron Optics 244 (2021) 167621

Contents lists available at ScienceDirect

Optik

journal homepage: www.elsevier.com/locate/ijleo

Synthesis of silver nanoparticles using chemical reduction techniques for Q-switcher at 1.5 μm region

Muhammad Quisar Lokman [a,*], Muhammad Farid Mohd Rusdi [b], Ahmad Haziq Aiman Rosol [b], Fauzan Ahmad [a,*], Suhaidi Shafie [c], Hafizal Yahaya [a], Rizuan Mohd Rosnan [d], Mohd Azizi Abdul Rahman [a], Sulaiman Wadi Harun [b]

[a] Malaysia-Japan International Institute of Technology (MJIIT), Universiti Teknologi Malaysia, Jalan Sultan Yahya Petra, 54100 Kuala Lumpur, Malaysia
[b] Photonics Engineering Laboratory, Department of Electrical Engineering, Faculty of Engineering, University of Malaya, 50603 Kuala Lumpur, Malaysia
[c] Institute of Advance Technology, Universiti Putra Malaysia (UPM), 43400 Serdang, Selangor, Malaysia
[d] Jeol (Malaysia) Sdn. Bhd., 47301 Petaling Jaya, Selangor, Malaysia

ARTICLE INFO

Keywords:
Silver nanoparticles
Saturable absorber
Q-switched
Erbium-doped fibre laser

ABSTRACT

This research investigated the generation of passively Q-switched erbium (Er)-doped fibre laser using silver nanoparticles/poly (vinyl alcohol) (Ag/PVA) as a saturable absorber (SA). The Ag nanoparticles were synthesised via the chemical reduction technique. The Ag/PVA film based SA was fabricated by blending Ag nanoparticles powder into the PVA suspension, then left to dry at ambient to develop a free-standing SA film. Next, the Ag/PVA film was sandwiched in between two FC/PC fibre ferrules and integrated into the laser cavity for Q-switched pulse generation. The result shows that the Q-switched pulsed laser achieved pulse energy and peak power of 128.04 nJ and 21.34 mW at the maximum pump power of 107.1 mW. A signal-to-noise ratio (SNR) value of 66.23 dB was obtained at a frequency of 66.23 kHz proving that it is an excellent candidate as a SA material for Q-switched generation in future large-scale manufacturing.

1. Introduction

The past decade has seen the rapid development of Q-switched laser sources in many industries and scientific research fields due to their versatile applications, such as communication, material processing, medical, non-linear optics, and remote sensing [1–5]. In Q-switching operations, the laser cavity loss switches from a high value during off-time to a low value during on-time. The Q-factor is described as the capacity to store light energy or ratio between the stored and loss energies after each round-trip in the cavity [6]. Typically, Q-switched laser generates short pulses from a microsecond to nanosecond regime with a low repetition rate in of range. The Q-switched laser pulse can be achieved either through active or passive techniques, where active techniques require external modulation devices such as acousto- or electro-optic modulators to modulate the cavity loss. However, active techniques are too expensive and complex to be used for the Q-switched laser system in real-life applications [7]. Therefore, the passive technique has been introduced and has shown inherent advantages over the active technique, including a compact, flexible, and simple laser system [8]. In recent years, there has been increasing interest in SA using the generation of passive Q-switched laser generation. Until now, numerous

* Corresponding authors.
E-mail addresses: muhammadquisar@gmail.com (M.Q. Lokman), fauzan.kl@utm.my (F. Ahmad).

https://doi.org/10.1016/j.ijleo.2021.167621
Received 1 April 2021; Received in revised form 8 July 2021; Accepted 9 July 2021
Available online 10 July 2021

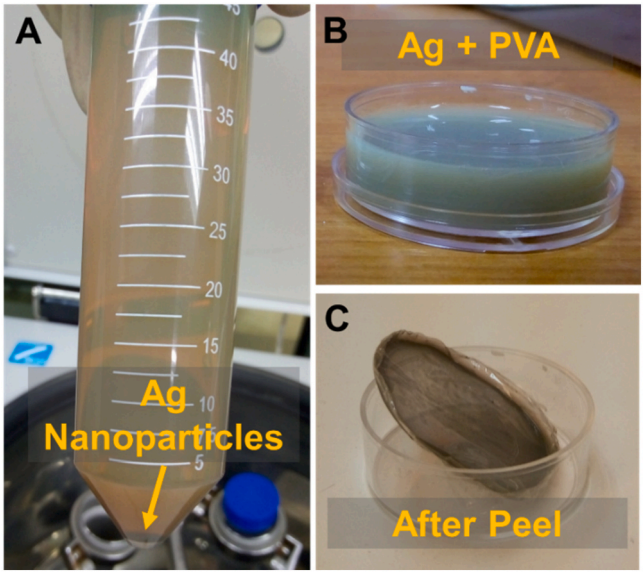

Fig. 1. Preparation of Ag/PVA SA (a) is the Ag colloidal after 6000 rpm centrifugation for 30 min, the Ag nanoparticles separated from colloidal solution (b) addition of Ag into PVA solution and (c) after 3 days, the Ag/PVA film was dried and peeled.

nanomaterials have been demonstrated as efficient SA materials in Q-switched fibre laser, including carbon nanotubes [9], graphene [10], transition metal dichalcogenides [11], topological insulator [12], transition-metal oxides [13], rare-earth oxides [14] and black-phosphorus [15], MXenes [16].

Recently, noble-metal nanoparticles including gold (Au), silver (Ag), and copper (Cu) have been drawing considerable interest due to their attractive optical property [17–19]. Notably, most SAs that are based on noble-metal nanoparticles for Q-switched generation are focused on Au nanoparticles, especially in ytterbium (Yb-), erbium (Er-) and thulium (Tm-) doped fibre laser [20–22]. Little attention has been paid to the role of Ag as a SA for Q-switched fibre lasers. Compared to the other metal nanoparticles, Ag has large and ultrafast third-order nonlinearities and the absorption spectrum could be extended to 1400 nm [23]. Besides, Ag has also been able to improve the fluorescence intensity around 1.53 μm due to the enhancement of the local electric field induced by localised surface plasmon resonance of Ag [24]. In addition, Ag (or plasmonic materials) possess a strong transient photobleaching behaviour (saturable absorption) in a subpicoseconds under short pulse excitations in the resonance spectral region as compared to other traditional SA. The reported third order susceptibility (χ^3) is roughly around 10^{-10} esu shows that Ag can be used as ideal SA for laser pulse generation [25]. Previous investigation in Ag-based SA had focused on optical deposition on the surface of fibre ferrule [26], and the electron beam evaporation (EBE) process [27] was used to integrate into the laser cavity. In an optical deposition, the process induces large scattering loss, and the process itself is quite tedious as many factors can influence the required optical power to make Ag adhere to the ferrule facets [6]. EBE process also has poor uniformity in the deposition if no masking is used in the process and there is limited scalability at reduced utilisation and deposition rates [28]. There are many deposition techniques of SA materials to be integrated in laser cavity [29], however, to be embedded with a host polymer is the preferred technique. Embedded Ag in PVA can effectively protect the Ag from other contaminants that can degrade the SA [30]. There are few host polymers that have been used in SA fabrication, such as poly (ethylene oxide) [31], PVA [9], poly (methyl methacrylate) [32], poly (dimethylsiloxane) [33] and chitosan [11]. However, PVA is preferable since PVA does not exhibit strong optical absorption at 1030 nm and 1558 nm [34]. Besides, it is selected due to its solvent compatibility (water-soluble), ease of fabrication (room temperature fabrication), robustness, flexibility (high tensile and not brittle) [34] and no strong chemical was used during the preparation that can damage the Ag nanoparticles [35].

In this paper, the generation of Q-switched Er-doped fibre laser using Ag/PVA SA is reported. The Ag nanoparticles were synthesised by using the chemical reduction method, where tri-sodium citrate was selected as a reducing agent. The Ag nanoparticles were mixed with PVA solution to develop a free-standing SA. The Ag/PVA was integrated into the laser cavity for Q-switched pulse generation.

2. Methodology

2.1. Preparation and characterisation of Ag/PVA SA

The colloidal Ag nanoparticles were synthesised through chemical reduction methods following the procedure from our previous report [36]. To prepare the Ag/PVA SA, the Ag nanoparticles were collected by centrifugation at 6000 rpm for 30 min to separate the Ag and excess reducing agent [see Fig. 1(a)]. The colloidal Ag was centrifuged three times and each time, Ag was replenished with deionised (DI) water to ensure the excess was completely removed. The aqueous PVA solution was prepared by adding 0.5 g PVA

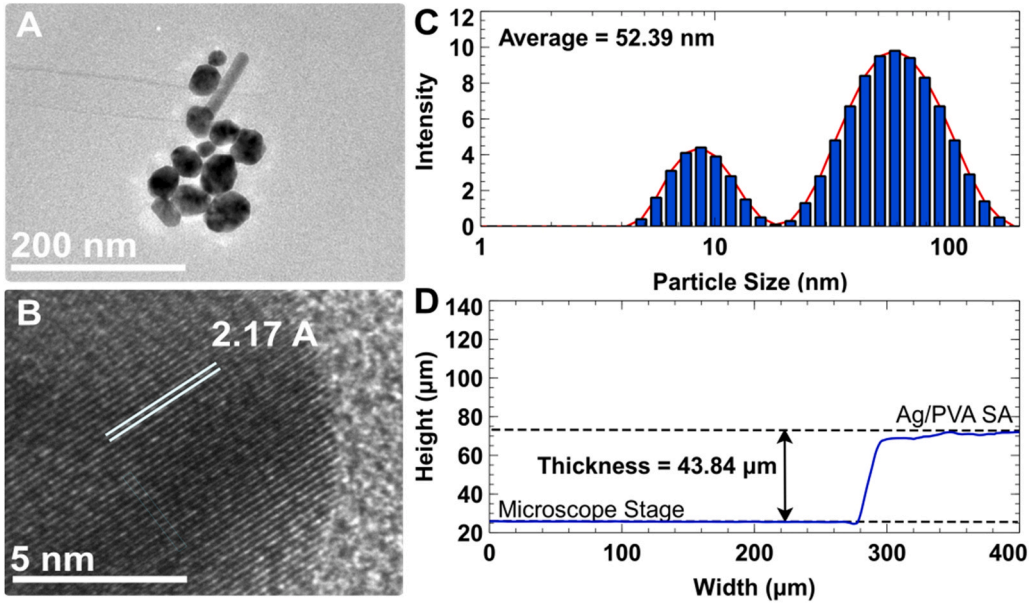

Fig. 2. (a) TEM, (b) high resolution image of synthesised Ag nanoparticle, (c) particle distribution and (d) thickness profile of Ag/PVA SA with thickness of 43.84 μm.

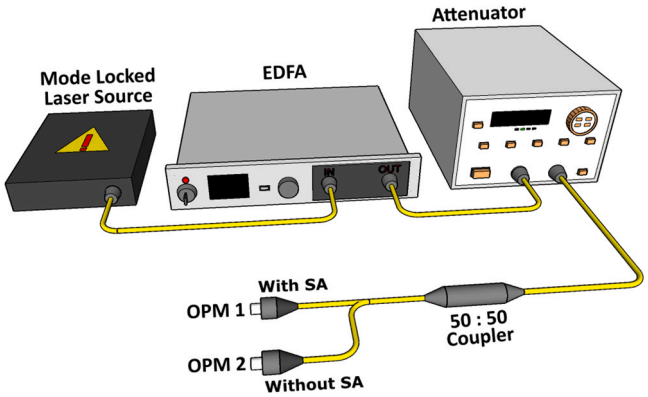

Fig. 3. Schematic diagram of balanced twin-detector for non-linear transmission. OPM 1 is with SA and OPM 2 without SA.

powder (40,000 MW, Sigma Aldrich) into 60 mL of DI water and heated at 145 °C until the powder completely dissolved. After that, Ag was added into PVA solution at one to five ratio (1:5, mg:mL) and ultra-sonicated for an hour, followed by stirring for 3 h. Lastly, the Ag/PVA solution was decanted into a petri dish and left to dry in the desiccator cabinet for 3 days as shown in Fig. 1(b). The film was carefully peeled to develop a free-standing film based SA and kept in the vacuum bag.

The transmission electron microscopy (TEM; JEOL, JEM-2100F) images in Fig. 2(a) represents the morphology and Fig. 2(b) depicts the high-resolution image to measure lattice fringes of synthesised Ag. Before analysis of TEM, the Ag was added into DI water at a ratio of 1:10 (mg:mL) and ultra-sonicated for 30 min, before being dropped onto a carbon lacey/copper grid. The TEM images show most of the Ag as quasi-spherical and monodispersed. The crystalline nature of a single particle was further studied by measuring the lattice spacing. The lattice spacing of synthesised Ag is 2.17 Å which corresponds to the (200) plane of Ag [37]. This shows that $AgNO_3$ is successfully reduced to Ag^+ ions by tri-sodium citrate and resulting formation of Ag cluster.

Fig. 2(c) shows the particle size distribution of synthesised Ag using dynamic light scattering (Malvern, ZSP-5600). It is shown that the Ag nanoparticles ranged around 5–100 nm. The slow reaction rate of the chemical reduction method contributes to the reactions and particle sizing range from 50 to 100 nm [38]. Particularly, when the particle seeds are formed from the reduction of Ag^+ by tri-sodium citrate, the remaining anion can complex to the metal surface decreasing the amount of citrate available in the bulk to further reduce more Ag^+. Therefore, fewer new seeds are reduced, and the initial particles begin to grow via Ostwald ripening, in which larger ones will continue to grow compared to the smaller ones [38,39]. However, in this experiment, the two distribution peak were observed. The Ag can be distributed uniformly by stabilising with poly (vinyl pyrrolidone) [40].

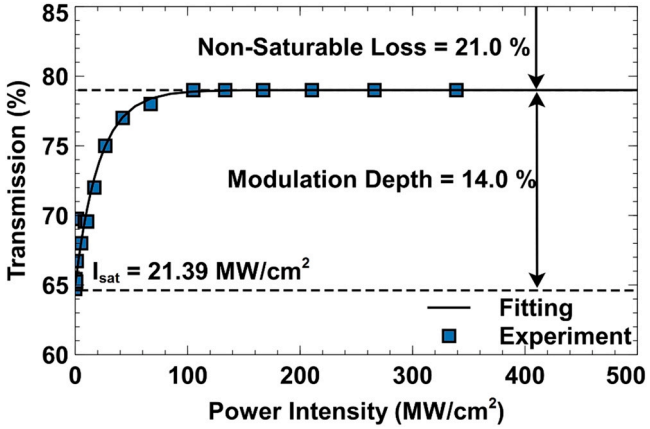

Fig. 4. Nonlinear transmission characteristic of Ag/PVA SA using the balanced twin-detector method.

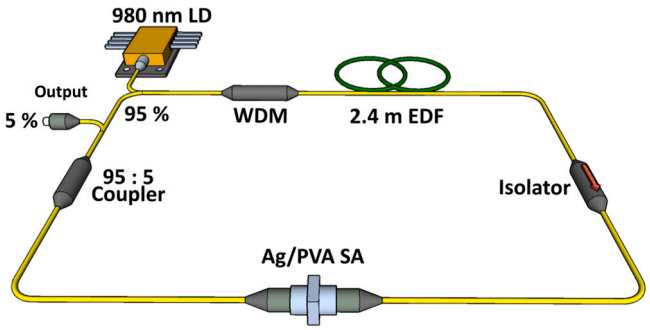

Fig. 5. Schematic of the Q-switched Er-doped fibre laser. LD, laser diode; WDM, wavelength division multiplexer; EDF, Erbium-doped fibre.

Fig. 2(d) shows the thickness profile of free-standing Ag/PVA SA film which was measured using a 3D laser scanning microscope (Olympus, OLS 4100). The thickness was measured by the difference in height of the SA and microscope stage. The measured thickness is around 43.84 μm which is consistent with other reported film thickness of around 50 μm [41].

2.2. Non-linear transmission setup

The non-linear transmission analysis was carried out in the experiment, to obtain the non-linear optical response of Ag/PVA SA. Fig. 3 shows the schematic setup for non-linear transmission using the balanced twin-detector technique. The setup comprises self-started mode-locked laser sources with a centre wavelength of 1555 nm and pulse width of 1 ps with a repetition rate of 15 MHz, and pre-amplified by using erbium-doped fibre amplifier (EDFA; Keopsys, CEFA-C-PB-LP), variable optical attenuator (Anritsu, MN9610B) was employed to adjust the input optical power into Ag/PVA film based SA. After that, 50% of the pre-amplified light was passed through the Ag/PVA SA, while the other remaining 50% was monitored as a reference. Both output power was recorded using an optical power meter. The data were fitted using the transmission fitting equation [27].

Fig. 4 shows the non-linear transmission of Ag/PVA SA as a function of power intensity. The modulation depth of the Ag/PVA SA is 14.0% and a non-saturable loss of 21.0%. The initial transmission ratio of 65.0% with a saturation intensity power of 21.39 MW/cm^2. The achieved modulation depth from this experiment is comparable to the other previous study report [26,27]. It is important to achieve large modulation for strong pulse shaping and stable Q-switching operation. However, the non-saturable loss is considerably high for Ag/PVA SA causing a high-power loss due to the low repetition rate of mode-locked input. The non-saturable loss can be reduced by using a stable femtosecond mode-locked input [27].

2.3. Q-switched Er-doped fibre laser setup

To demonstrate the potentiality of using Ag/PVA SA for Q-switched fibre laser, the all fibre-integrated Er-doped fibre laser cavity in a ring configuration was constructed as shown in Fig. 5. A 2.4 m Er-doped active fibre (FiberCore, I-25) with a peak absorption of 45 dB/m at 1531 nm was co-pumped by a 980 nm laser diode (LD) via wavelength-division multiplexer (WDM). An isolator was included in the cavity to avoid light propagation from entering the formation of the standing waves that may damage the LD. The fused-fibre output coupler (95:5) that was employed, was at 5% for output diagnostics to observe spectral characteristics, pulse train,

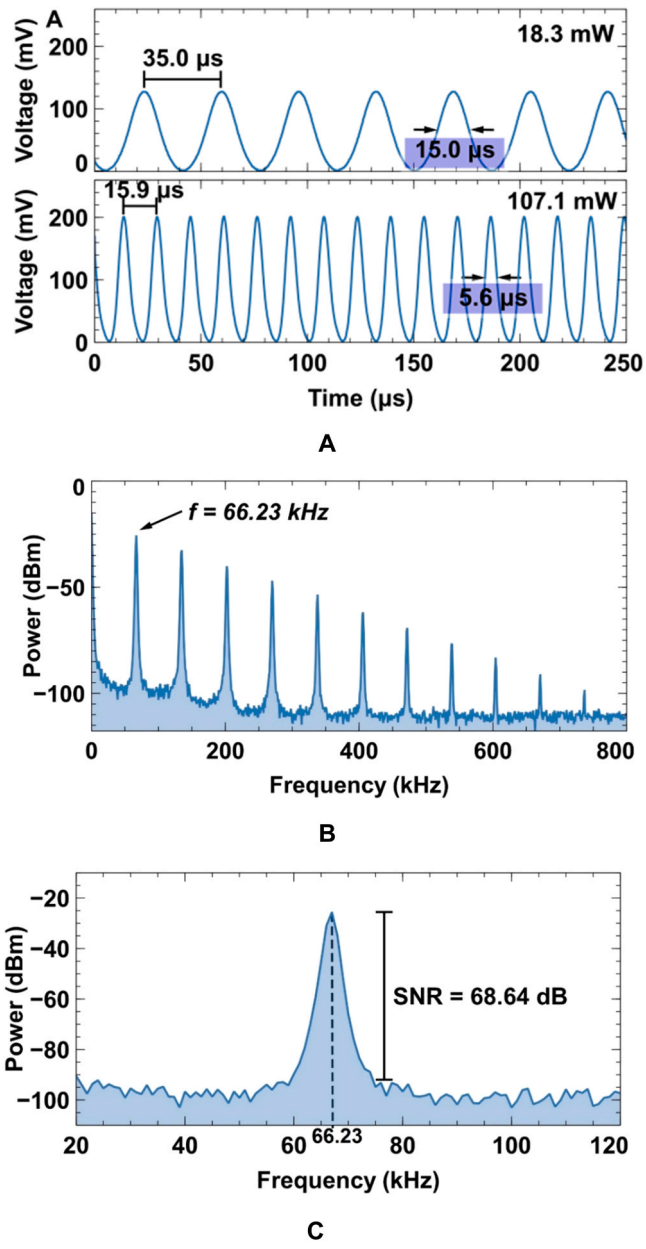

Fig. 6. (a) Typical pulse train at pump power 18.3 mW and 107.1 mW, and (b) RF spectrum with 11th harmonic peaks and (c) fundamental frequency with SNR of 68.64 dB at maximum pump power 107.1 mW.

and signal-to-noise ratio (SNR). Meanwhile, the other 95% were kept resonating in the cavity. The spectral characteristic of the Q-switched pulse was obtained using an optical spectrum analyser (OSA; Yokogawa, AQ6370B) with a resolution of 0.02 nm. The Q-switched pulse train was observed using a digital oscilloscope and SNR was acquired using a radio-frequency spectrum analyser (RFSA; Anritsu, MS2683A). Both types of equipment were connected using a 1.2 GHz InGaAs photodetector (Thorlabs, DET01CFC). The free-standing Ag/PVA SA was integrated into the laser cavity by sandwiching a 1 mm^2 in between two fibre patch cords with the aid of index matching gel. The total length of the laser cavity was around 13.4 m and all the components were connected by direct splicing with a total cavity splicing loss of 0.13 dB.

3. Results and discussions

The continuous wave (CW) lasing was first obtained when the pump power approached 12.7 mW. The low pump pomp power during the CW operation showed that low cavity losses were due to direct splicing between the optical components [40]. In addition,

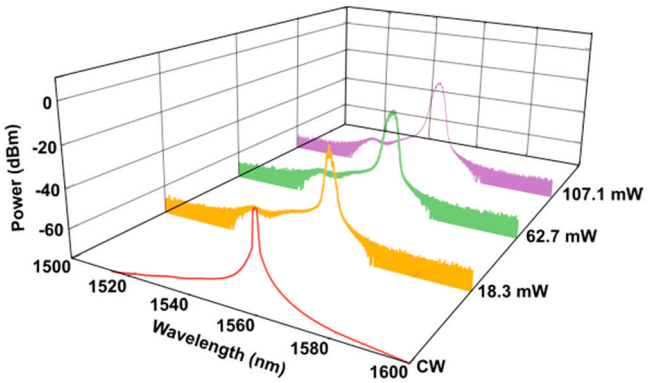

Fig. 7. Optical spectrum trace from OSA at pump power 18.3 mW, 62.7 mW, and 107.1 mW, and CW mode.

the obtained initial pump power for Q-switching seemed lower than the other reported works based on Ag SA [26,27,42,43]. The self-operated Q-switching generated a stable pulse and was obtained at the pump power of 18.3 mW, as the Ag/PVA SA was integrated into the laser ring cavity. By further increasing the pump power above 107.1 mW, the Q-switched pulses observed started to fluctuate followed by diminishing pulses which were caused by over-saturation of SA. Markedly, the stable pulse re-appeared when the Ag/PVA SA was tuned from 18.3 mW to 107.1 mW without any significant fluctuations observed in the oscilloscope. Furthermore, to validate whether the Q-switching was induced by the Ag/PVA SA, the Ag/PVA SA was replaced with the pure PVA film and integrated into the ring cavity. In this instance, no pulse train was detected, even though the pump power was tuned to the maximum. Fig. 6(a) displays the typical pulse train and single pulse envelop of the Q-switch at 18.3 mW and 107.1 mW. The pulses showed symmetrical Gaussian-like profiles and yet amplitude modulation was not observed in the pulse train. The shortest pulse width at FWHM at around 5.6 μs was obtained at the maximum pump power of 107.1 mW with a pulse-to-pulse interval of 15.9 μs which corresponded to the repetition rate of 66.23 kHz. As shown in Fig. 6(a), the interval between two pulses was closer and pulse width at FWHM decreased as the pump power increased.

Fig. 6(b) displays the frequency domain spectrum retrieved from the radio-frequency spectrum analyser (resolution bandwidth, RBW = 1000 Hz) and it corresponded to SNR at a fundamental frequency of 66.23 kHz as shown in Fig. 6(c). To investigate the laser stability SNR was measured by subtracting the peak and the pedestal power of the fundamental frequency. The SNR was at a maximum pump power of 107.1 mW when the fundamental frequency was 68.64 dB. This high SNR value that exceeds 30 dB indicated that the Q-switched pulsed laser operated at good stability. The frequency spectrum shows 11th harmonic peaks and gradually decreased at every consecutive harmonic peak before it completely disappeared indicating that the Q-switched operates in broad pulse width. Furthermore, the fundamental and harmonic frequency peak existed within the 800 kHz span range and no external spectrum component was present over 800 kHz.

Fig. 7 shows the spectral characteristic of CW lasing retrieved from optical spectrum analyser that occurred without the integration of Ag/PVA SA into the laser cavity and Q-switched pulse under different pump power. The CW was achieved at a pump power of 12.7 mW with a centre wavelength of 1561 nm and a 3 dB bandwidth of 1.5 nm. Whereas, at the maximum pump power of 107.1 mW, the Q-switched centre wavelength was at 1558.14 nm with a 3 dB bandwidth of 2.0 nm. As the Ag/PVA SA was integrated into the laser cavity, the centre wavelength that was observed became slightly blue-shifted caused by CW to Q-switched transition due to the absorption of light by Ag/PVA SA. Also, non-linear effects of the fibre and Ag/PVA SA can induced the broadening of 3 dB bandwidth.

Fig. 8(a) shows the repetition rate and pulse width as a function of the pump power. The repetition rate showed a positive correlation, meanwhile an exponentially negative rate was observed for pulse width as pump power increased. This showed the typical Q-switched operation. Unlike the mode-locking operation, the repetition rate of Q-switched operation depends on the pump power, not determined by the length of the laser cavity [27]. With the increase of pump power, more electrons could excite and accumulated at the upper level. Therefore, the rise time and falling time of pulse trains became simultaneously shorter. This can lead to a reduction of pulse width and an increase in the repetition rate [12]. Also, in Fig. 8(a) the achieved repetition rate was increased from 28.57 kHz to 66.23 kHz with a decreasing pulse width of 15.00 μs to 5.60 μs when the pump power was tuned from 18.3 mW to 107.1 mW. Fig. 8(b) shows the average output power in the range of 0.899–8.48 Mw recorded using optical power meter. Fig. 8(c) shows the single pulse energy and instantaneous peak power of Ag/PVA SA at pump power tuned from 18.3 mW to 107.1 mW. At a maximum pump power of 107.1 mW, the calculated pulse energy was 128.04 nJ. The instantaneous peak power at a maximum pump power of 107.1 mW was 21.37 mW. It was also possible that the pulse energy and peak power of the Q-switched fibre laser could increase if the Ag/PVA SA was optimised. The non-saturable loss of the SA should be as low as possible to reduce the power losses during the saturable absorption process and the modulation depth had to be higher to generate a shorter and intense pulse width.

In the proposed work, Ag nanoparticles were synthesised by using the chemical reduction method and embedded in the PVA polymer matrix where they appeared to generate Q-switched laser with high peak power and pulse energy at low threshold input pump power. This approach offers low-cost fabrication in terms of raw materials and deposition equipment compared to prior works of Ag-based SA. In addition, the proposed synthesised Ag nanoparticles can function as a tuneable Q-switched laser by varying the Ag nanoparticle sizes by using different amounts of reducing agent, for example, tri-sodium citrate as seen in this experiment. The

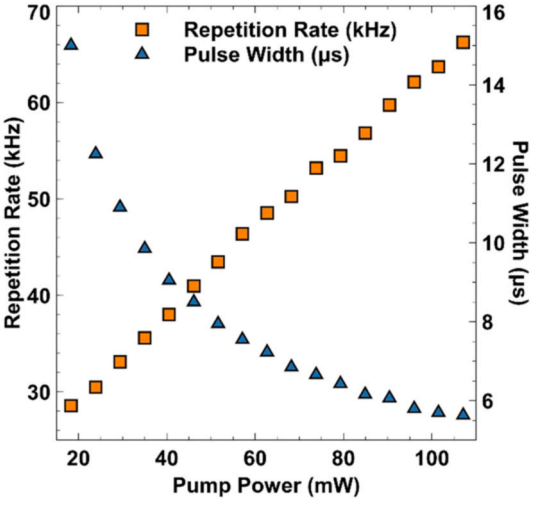

A

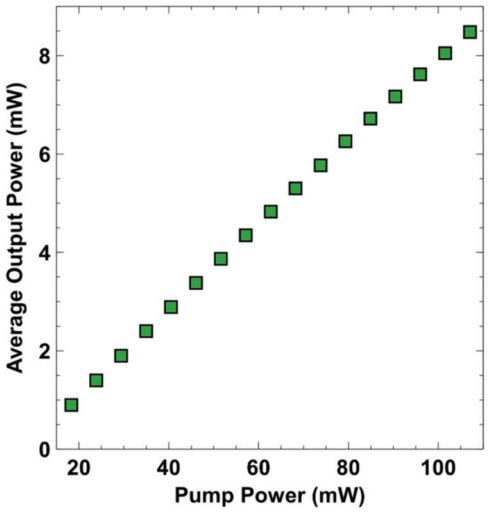

B

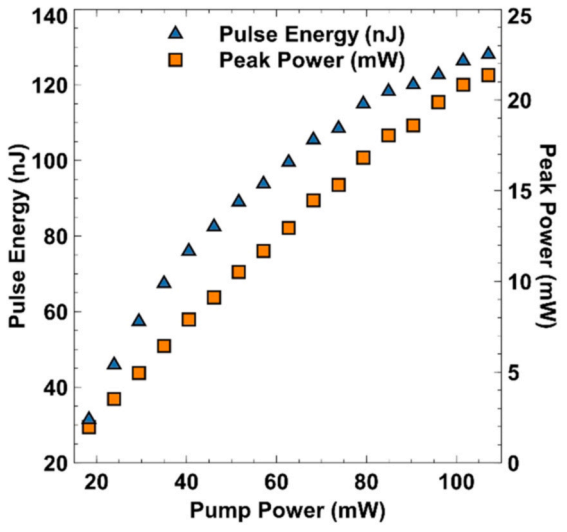

C

(caption on next page)

Fig. 8. (a) Repetition rate and pulse width, (b) average output power, and (c) instantaneous peak power and single pulse energy as a function of the pump power.

Table 1
Laser performance comparison of previous study on Ag nanoparticles based SA for Q-switched EDFL.

Metal	Method	Mod. depth (%)	Initial pump power (mW)	Rep. rate (kHz)	Pulse width (μs)	Max pulse energy (nJ)	Max peak power (mW)	SNR (dB)	Ref.
Ag	Optical Deposition	18.5	19.9	17.9–58.5	11.4–2.4	132	None	None	[26]
	Electron Beam Evaporation	19.0	29.4	39.8–65.4	11.6–6.7	146.7	20.5	67.52	[27]
	MTMS	31.6	20.0	13.8–39.2	5.9–3.4	~4.2	~ 2.0	46.2	[42]
	Ag/RGO Embedded in PVA	30.0	27.4	10.05–76.63	8.80–1.38	11.14	3.32	53.4	[43]
	Embedded in PVA	14.0	18.3	28.57–66.23	15.0–5.6	128.04	21.37	68.64	This Work
Au	Electron Beam Evaporation	None	17.3	24.34–88.11	17.58–4.52	32.9	None	57.42	[45]
Cu	Electron Beam Evaporation	36.0	26.1	41.7–101.2	10.19–4.28	18.37	4.29	50.9	[46]

Notes: MTMS – Methyltrimethoxysilane; RGO – Reduced graphene oxide.

nanoparticle sizes are an important factor that can influence the absorption of surface plasmon resonance (SPR) by injecting light that can tune the optical spectrum to a different wavelength [44]. Moreover, the sizes of the nanoparticles can also influence the modulation depth of the SA. In these cases, the larger Ag nanoparticles size can absorb more of the injected light. Large modulation depth can affect the pulse shaping, where reduction of pulse width will occur [10]. The comparison is presented in Table 1.

4. Conclusion

This work demonstrated the Q-switched Er-doped fibre laser by using Ag/PVA as SA. The Ag nanoparticles were synthesised by using a chemical reduction method and tri-sodium citrate was used as a reduction agent. To develop free-standing Ag/PVA SA, the Ag nanoparticles were added into the PVA solution and left to dry at ambient temperature for 3 days. Then, the Ag/PVA was integrated between two FC/PC fibre ferrules and tested for Q-switched pulse generation. The results showed that the modulation depth of the SA was at 14.0% with a non-saturable loss of 21.0%. The SA generated a pulse at 18.3 mW with maximum pulse energy and peak power of 128.04 nJ and 21.37 mW. The Q-switched laser operated at centre wavelength 1558.14 nm with 68.64 dB of SNR. This showed that the synthesis Ag/PVA using chemical reduction approach and embedded in PVA has a potential Q-switched pulse fibre laser with high pulse energy and SNR. The potential application of the fabricated Ag based passive SA, for example, laser material processing, medical, and communication systems.

Declaration of Competing Interest

The authors declare that they have no known competing financial interests or personal relationships that could have appeared to influence the work reported in this paper.

Acknowledgement

This work was supported by the Universiti Teknologi Malaysia [UTMHR, 2243.08G99]. The author thanks to Photonics Engineering Laboratory, University of Malaya for fibre laser equipment and facility. Also would like to thank the Postdoctoral Fellowship from Universiti Teknologi Malaysia.

References

[1] S.V. Garnov, V.I. Konov, T. Kononenko, V.P. Pashinin, M.N. Sinyavsky, Microsecond laser material processing at 1.06 μm, Laser Phys. 14 (2004) (2004) 910–915.
[2] C. Evangelatos, G. Tsaknakis, P. Bakopoulos, D. Papadopoulos, G. Avdikos, A. Papayannis, G. Tzeremes, Actively Q-switched multisegmented Nd: YAG laser pumped at 885 nm for remote sensing, IEEE Photonics Technol. Lett. 26 (2014) 1890–1893.
[3] T. Omi, R. Yamashita, S. Kawana, S. Sato, Z. Naito, Low fluence Q-switched Nd: YAG laser toning and Q-switched ruby laser in the treatment of melisma, Laser Ther. 21 (2012) 1–15.
[4] S. Pavlova, M.E. Yagci, S.K. Eken, E. Tunckol, I. Pavlov, High power microsecond fiber laser at 1.5 μm, Opt. Express 28 (2020) 18368–18375.
[5] N. Cui, F. Zhang, Y. Zhao, Y. Yai, Q. Wang, L. Dong, H. Zhang, S. Liu, J. Xu, H. Zhang, The visible nonlinear optical properties and passively Q-switched laser application of a layered $PtSe_2$ material, Nanoscale 12 (2020) 1061–1066.
[6] M.A. Ismail, S.W. Harun, H. Ahmad, M.C. Paul, Passive Q-switched and mode-locked fiber lasers using carbon-based saturable absorbers, IntechOpen, Rijeka, 2016.
[7] R. Paschotta, Field Guide to Laser Pulse Generation, SPIE Press, Bellingham, 2008.

[8] U. Keller, Recent developments in compact ultrafast lasers, Nature 424 (2003) 831–838.
[9] D. Sun, X. Xu, J. Chen, L. Sun, S. Chu, S. Ruan, Passively Q-switched ytterbium-doped fiber laser based on a SWCNT@ AFI saturable absorber, Opt. Laser Technol. 136 (2021), 106781.
[10] R. Zhang, J. Wang, M. Liao, X. Li, P.W. Kuan, Y. Liu, Y. Zhou, W. Gao, Tunable Q-switched fiber laser based on a graphene saturable absorber without additional tuning element, IEEE Photonics J. 11 (2019) 1–10.
[11] H. Hou, T. You, Q. Zhou, M. Liu, Y. Ouyang, X. Liu, W. Liu, Q-switched all-fiber laser based on titanium trisulfide, Optik 205 (2020), 164234.
[12] D.P. Sudas, E.A. Savelyev, P.I. Kuznetsov, K.M. Golant, Features of repetitively-pulsed oscillation of an erbium fiber laser with a saturable absorber Bi_2Te_3 covered by silicone at various temperatures, Phys. Scr. 96 (2021), 045501.
[13] N.M. Yusoff, C.A.C. Abdullah, M.A. Hadi, E.K. Eng, H.K. Lee, N.Z. Abidin, N.S. Rosli, M.A. Mahdi, Low threshold Q-switched fiber laser incorporating titanium dioxide saturable absorber from waste material, Optik 218 (2020), 164998.
[14] N.F. Zulkipli, A.A.A. Jafry, R. Apsari, F.S.M. Samsamnun, M. Batumalay, M.I.M.A. Khudus, H. Arof, S.W. Harun, Generation of Q-switched and mode-locked pulses with Eu_2O_3 saturable absorber, Opt. Laser Technol. 127 (2020), 106163.
[15] J. Liu, Y. Chen, Y. Li, H. Zhang, S. Zheng, S. Xu, Switchable dual-wavelength Q-switched fiber laser using multilayer black phosphorus as a saturable absorber, Photonics Res. 6 (2018) 198–203.
[16] A.A.A. Jafry, A.R. Muhammad, N. Kasim, A.H.A. Rosol, M.F.M. Rusdi, N.N.N. Ab Alim, S.W. Harun, P. Yupapin, Ultrashort pulse generation with MXene $Ti_3C_2T_x$ embedded in PVA and deposited onto D-shaped fiber, Opt. Laser Technol. 136 (2021), 106780.
[17] D. Wu, H. Lin, Z. Cai, J. Peng, Y. Cheng, J. Weng, H. Xu, Saturable absorption of copper nanowires in visible regions for short-pulse generation, IEEE Photonics J. 8 (2016) 1–7.
[18] C. Zheng, W. Li, W. Chen, X. Ye, Nonlinear optical behavior of silver nanopentagons, Mater. Lett. 116 (2014) 1–4.
[19] P.K. Jain, X. Huang, I.H. El-Sayed, M.A. El-Sayed, Review of some interesting surface plasmon resonance-enhanced properties of noble metal nanoparticles and their applications to biosystems, Plasmonics 2 (2007) 107–118.
[20] H. Wu, J. Song, J. Wu, J. Xu, H. Xiao, J. Leng, P. Zhou, Concave gold bipyramid saturable absorber based 1018 nm passively Q-switched fiber laser, IEEE J. Sel. Top. Quantum Electron. 24 (2017) 1–6.
[21] Z. Kang, X. Guo, Z. Jia, Y. Xu, L. Liu, D. Zhao, W. Qin, Gold nanorods as saturable absorbers for all-fiber passively Q-switched erbium-doped fiber laser, Opt. Mater. Express 3 (2013) 1986–1991.
[22] A.R. Muhammad, R. Zakaria, M.T. Ahmad, P. Wang, S.W. Harun, Pure gold saturable absorber for generating Q-switching pulses at 2 μm in Thulium-doped fiber laser cavity, Opt. Fiber Technol. 50 (2019) 23–30.
[23] F. Chen, J. Cheng, S. Dai, Z. Xu, W. Ji, R. Tan, Q. Zhang, Third-order optical nonlinearity at 800 and 1300 nm in bismuthate glasses doped with silver nanoparticles, Opt. Express 22 (2014) 13438–13447.
[24] Y. Qi, Y. Zhou, L. Wu, F. Yang, S. Peng, S. Zheng, D. Yin, Silver nanoparticles enhanced 1.53 μm band fluorescence of Er^{3+}/Yb^{3+} codoped tellurite glasses, J. Lumin. 153 (2014) 401–407.
[25] V. Singh, Surface plasmon enhanced third-order optical nonlinearity of Ag nanocomposite film, Appl. Phys. Lett. 104 (2014), 111112.
[26] H. Guo, M. Feng, F. Song, H. Li, A. Ren, X. Wei, Y. Li, X. Xiu, J. Tian, Q-switched erbium-doped fiber laser based on silver nanoparticles as a saturable absorber, IEEE Photonics Technol. Lett. 28 (2015) 135–138.
[27] M.Q. Lokman, S.F.A.Z. Yusoff, F. Ahmad, R. Zakaria, H. Yahaya, S. Shafie, R.M. Rosnan, S.W. Harun, Deposition of silver nanoparticles on polyvinyl alcohol film using electron beam evaporation and its application as a passive saturable absorber, Results Phys. 11 (2018) 232–236.
[28] A.S.H. Makhlouf, Current and Advanced Coating Technologies for Industrial Applications, Woodhead Publishing, Cambridge, 2011.
[29] M. Zhang, Q. Wu, F. Zhang, L. Chen, X. Jin, Y. Hu, Z. Zheng, H. Zhang, 2D black phosphorus saturable absorbers for ultrafast photonics, Adv. Opt. Mater. 7 (2019), 1800224.
[30] R. Saikia, P. Gogoi, P. Datta, Fabrication of Ag/PVA nanocomposites and their potential applicability as dielectric layer in thin film capacitor, J. Exp. Nanosci. 8 (2013) 194–202.
[31] A.H.H. Al-Masoodi, I.A. Alani, M.H.M. Ahmed, A.H. Al-Masoodi, A.A. Alani, P. Wang, S.W. Harun, Cobalt oxide nanocubes thin film as saturable absorber for generating Q-switched fiber lasers at 1 and 1.5 μm in ring cavity configuration, Opt. Fiber Technol. 45 (2018) 128–136, 138-136.
[32] N.A. Aziz, Z. Jusof, M.Q. Lokman, M. Yasin, E. Hanafi, S.W. Harun, Q-switched erbium-doped fiber laser with graphene oxide embedded in PMMA film, Dig. J. Nanomater. Biostruct. 12 (2017) 325–330.
[33] E.I. Ismail, F. Ahmad, S. Shafie, H. Yahaya, A.A. Latif, F.D. Muhammad, Copper nanowires based mode-locker for soliton nanosecond pulse generation in erbium-doped fiber laser, Results Phys. 18 (2020), 103228.
[34] M. Zhang, G. Hu, G. Hu, R.C.T. Howe, L. Chen, Z. Zheng, T. Hasan, Yb-and Er-doped fiber laser Q-switched with an optically uniform, broadband WS_2 saturable absorber, Sci. Rep. 5 (2015) 17482.
[35] I.A. Ezenwa, N.A. Okereke, N.J. Egwunyenga, Optical properties of chemical bath deposited Ag_2S thin films, Int. J. Sci. Technol. 2 (2012) 101–106.
[36] M.Q. Lokman, S. Shafie, S. Shaban, F. Ahmad, H. Jaafar, R.M. Rosnan, H. Yahaya, S.S. Abdullah, Enhancing photocurrent performance based on photoanode thickness and surface plasmon resonance using Ag-TiO_2 nanocomposites in dye-sensitized solar cells, Materials 12 (2019) 2111.
[37] B.K. Mehta, M. Chhajlani, B.D. Shrivastava, Green synthesis of silver nanoparticles and their characterization by XRD, J. Phys. Conf. Ser. 836 (2017), 012050.
[38] Z.S. Pillai, P.V. Kamat, What factors control the size and shape of silver nanoparticles in the citrate ion reduction method, J. Phys. Chem. 108 (2004) 945–951.
[39] N.L. Pacioni, C.D. Borsarelli, V. Rey, A.V. Veglia, Synthetic Routes for the Preparation of Silver Nanoparticles, Springer, Cham, 2015.
[40] L. Gharibshahi, E. Saion, E. Gharibshahi, A.H. Shaari, K.A. Matori, Influence of Poly(vinylpyrrolidone) concentration on properties of silver nanoparticles manufactured by modified thermal treatment method, PLoS One 12 (2017), e0186094.
[41] H. Ahmad, M.F. Ismail, S.N.M. Hassan, F. Ahmad, M.Z. Zulkifli, S.W. Harun, Multiwall carbon nanotube polyvinyl alcohol-based saturable absorber in passively Q-switched fiber laser, Appl. Opt. 53 (2014) 7025–7029.
[42] H. Ahmad, N.E. Ruslan, M.A. Ismail, Z.A. Ali, S.A. Reduan, C.S.J. Lee, S.W. Harun, Silver nanoparticle-film based saturable absorber for passively Q-switched erbium-doped fiber laser (EDFL) in ring cavity configuration, Laser Phys. 26 (2016), 095103.
[43] H. Ahmad, H.S. Albaqawi, N. Yusoff, S.A. Reduan, C.W. Yi, Reduced graphene oxide-silver nanoparticles for optical pulse generation in ytterbium-and erbium-doped fiber lasers, Sci. Rep. 10 (2020) 1–11.
[44] D. Zhao, Y. Liu, J. Qiu, X. Liu, Plasmonic saturable absorbers, Adv. Photon. Res. (2021), 2100003.
[45] M.T. Ahmad, A.R. Muhammad, R. Zakaria, H.R.A. Rahim, K.S. Hamdan, H.H.M. Yusof, H. Arof, S.W. Harun, Gold nanoparticle based saturable absorber for Q-switching in 1.5 μm laser application, Laser Phys. 27 (2017), 115101.
[46] A.R. Muhammad, M.T. Ahmad, R. Zakaria, H.R.A. Rahim, S.F.A.Z. Yusoff, K.S. Hamdan, H. Arof, S.W. Harun, Q-switching pulse operation in 1.5-μm region using copper nanoparticles as saturable absorber, Chin. Phys. Lett. 34 (2017), 034205.